

Tracer Studies in Laboratory Beach Simulating Tidal Influences

Michel C. Boufadel, M.ASCE¹; Makram T. Suidan, M.ASCE²; and Albert D. Venosa³

Abstract: Bioremediation of oil spills on tidally influenced beaches commonly involves the addition of a nutrient solution to the contaminated region of the beach at low tide to stimulate the growth of indigenous oil-degrading bacteria. Maximizing the residence time of nutrients in the beach and subsequently their contact time with microorganisms is a main goal for successful bioremediation. Therefore, understanding the effects of the tide on water flow and solute transport in a beach is an essential task for designing a nutrient application strategy. We investigated these effects by conducting a tracer study in a laboratory beach simulating nutrient application on natural beaches. The study consisted of applying, at low tide, a conservative tracer solution onto the beach surface near the high-tide line and monitoring its movement in the beach subsurface. The tidal motion caused the applied plume to move downward and seaward. The downward movement occurred during rising tides, while the seaward movement occurred mainly during falling tides. The results indicate that nutrients should be applied at the high-tide line during low tides. Guidelines for scaling up the results to natural beaches are provided along with an example.

DOI: 10.1061/(ASCE)0733-9372(2006)132:6(616)

CE Database subject headings: Oil spills; Nutrients; Biological treatment; Beaches.

Introduction

Bioremediation is an emerging technology for restoration of oil-contaminated beaches (Merlin et al. 1995). One implementation of bioremediation involves the addition of nutrients, such as nitrogen and phosphorus, that can limit the growth rate of indigenous hydrocarbon-degrading bacteria. For example, recent biodegradation studies demonstrated that a nutrient-nitrogen concentration of approximately 2.0 mg/L is sufficient for the maximum growth of hydrocarbon-degrading microorganisms (Venosa et al. 1996; Boufadel et al. 1999a). Note that these two studies assume that the remaining nutrients are not limited.

The effectiveness of biostimulation depends on contact between the added nutrients and oil in the polluted zone (the bioremediation zone), which is usually less than 25 cm deep (Rosenburg et al. 1992). Ideally, nutrient concentrations in contact with the oil should be sufficient to support maximal growth rate of the oil-degrading bacteria, and this concentration must be maintained for the longest possible time. Therefore, maximizing the residence time of the nutrients in the contaminated zone of the beach is an important goal for bioremediation.

Many approaches have been developed to maintain contact between oil and nutrients, including lipophilic and slow-release methods for the nutrients. However, most slow-release and many lipophilic fertilizers rely on dissolution of the nutrients into the aqueous phase before they can be used by hydrocarbon degraders (Safferman 1991). Thus, design of effective oil bioremediation strategies and nutrient delivery systems requires an understanding of the transport of water-soluble fertilizer in the beach.

Dissolved nutrients are expected to move with the water in the beach sand. Water flow through the porous matrix of a beach is driven by a combination of three main factors. The first factor is the presence of a difference in density between freshwater and saltwater. Under steady-state hydraulic boundary conditions (i.e., no waves or tide), incoming freshwater floats above a saltwater wedge and exits the beach (Glover 1959; Henry 1964; Frind 1982; Galeati et al. 1992; Boufadel 2000). Therefore, the saltwater wedge acts as an impermeable boundary for the freshwater, forcing it to be funneled toward the beach surface.

The second factor that affects water flow in beaches is the waves, which operate through the mechanism of runup-rundown (Riedl et al. 1972; Brown and McLachlan 1990). At wave runup, water enters the beach, and at wave rundown, water moves seaward and exits the beach.

The third factor that influences groundwater flow in beaches is the tide, whose effect on the beach water table has been investigated by many researchers. Philip (1973) represented a beach as a vertical face and proved analytically that the average water table in the beach is higher than the average seawater level. A direct result of Philip's finding is that a tidally averaged seaward hydraulic gradient persists in the beach. Nielsen (1990) proved that the finding of Philip (1973) is also valid for naturally sloping beaches. Boufadel et al. (1998) reported laboratory model data (from the experimental setup used in this study, Fig. 1) and computer simulations for the rise and fall of water table due to tide. Their findings confirm those of Philip (1973) and Nielsen (1990).

¹Associate Professor, Dept. of Civil and Environmental Engineering, Temple Univ., Philadelphia, PA 19122 (corresponding author). E-mail: boufadel@temple.edu

²Professor, Dept. of Civil and Environmental Engineering, Univ. of Cincinnati, Ohio.

³U.S. Environmental Protection Agency, National Risk Management Research Laboratory, Cincinnati, Ohio.

Note. Discussion open until November 1, 2006. Separate discussions must be submitted for individual papers. To extend the closing date by one month, a written request must be filed with the ASCE Managing Editor. The manuscript for this paper was submitted for review and possible publication on November 30, 2004; approved on September 14, 2005. This paper is part of the *Journal of Environmental Engineering*, Vol. 132, No. 6, June 1, 2006. ©ASCE, ISSN 0733-9372/2006/6-616-623/\$25.00.

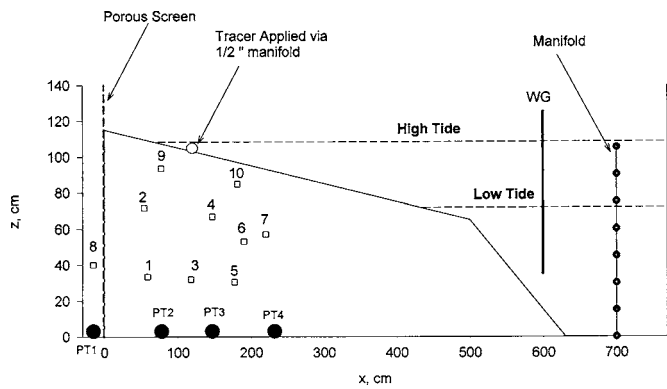


Fig. 1. Laboratory setup showing location of sensors. Pressure transducers were used to provide water table in beach; water level at sea side (righthand side of figure) was measured using a wave gauge; and hollow squares are conductivity meters used to measure concentration of NaCl

These three studies focused on the movement of the water table and did not consider the transport of solute in the beach.

Wrenn et al. (1997b) conducted a tracer study on a Delaware beach to simulate dissolved nutrient transport. They applied lithium onto the beach surface at low tide (as a lithium nitrate solution) to simulate the application of nutrient. This application strategy had also been used by Venosa et al. (1996) to bioremediate an intentional oil spill on a Delaware beach. Wrenn et al. (1997b) observed that the tracer is washed out from the intertidal zone (the section of the beach between the low tide and the high tide) within one tidal cycle. The beach that they investigated was subjected to waves, and they could not achieve a separate assessment of the effects of tide and waves. Wrenn et al. (1997a) reported preliminary results of tracer studies conducted on two beaches in Maine, one protected and one subjected to waves. They found that tide alone causes the washout of tracer to sea, and that waves greatly accelerate the washout.

In this work we study the effects of tides on beach flow and transport in a laboratory-scale model (Fig. 1) using sodium chloride (NaCl) as a conservative tracer. A solution of NaCl was applied onto the beach surface at low tide, simulating nutrient application. The water levels (WLs) and the salt concentrations were monitored at various locations in the laboratory beach. The results of this study provided information about beach flow and transport that can be used in other nutrient application strategies.

Laboratory Beach

Experimental Layout

The facility used in the experiment consisted of an 8 m long \times 2 m high \times 0.6 m wide carbon steel tank, as seen in Fig. 1. One of the long vertical sides (8 m \times 2 m) was made transparent by replacing the steel sheets with Plexiglas. The sand was positioned at a slope of 10% from a height of 115 to 65 cm and at 40% slope from 65 cm to zero, which resulted in a total horizontal sand coverage of about 630 cm. A screen made of expanded steel and fine mesh was installed 30 cm from the left wall to hold the sand and to allow water passage. The water volume to the left of the screen represents the landward water table, while the open water volume at the right side of the beach in Fig. 1 represents the sea.

Two sacrificial zinc plates were placed in the tank on both ends to reduce steel corrosion from the tank. Zinc was selected because it has a higher oxidation potential than steel.

Sand Properties

The sand used in the tank was coarse with a median size of 1.0 mm and a narrow particle size distribution, varying from 0.8 to 1.2 mm. These sand properties resulted in very little sand transport by suspension. Before the sand was placed in the tank, its porosity was measured as 0.38 by filling a 4 L beaker with well-drained sand and adding a sufficient amount of water to produce ponding conditions at the sand surface. The ratio of the volume of the added water to the apparent volume of the sand is, by definition, the porosity of the medium (Bear 1972). The sand was compacted in place using a concrete vibrator to eliminate water channeling. The porosity of the sand in the tank was estimated in situ by observing the settlement of the beach sand profile after compaction. The reduction in sand height in the beach was about 13%, resulting in a porosity of $(1 - 0.13) (0.38) = 0.33$.

The saturated hydraulic conductivity of the compacted sand was estimated in Boufadel et al. (1998) using Bayesian parameter estimation and was found to equal about 0.2 cm/s. The van Genuchten (1980) unsaturated parameters of the sand were estimated by the same procedure in Boufadel et al. (1998) and were found to equal $\alpha_v = 0.155 \text{ cm}^{-1}$ and $n_v = 3.5$. The inverse of α_v (equal to 6.45 cm herein) provides an estimate of the capillary fringe (zone of considerable moisture above the water table). The parameter n_v represents the pore-size distribution, and higher n_v values imply more uniform distributions. The estimated value of n_v falls on the high end of typical n_v values in natural systems, which range from 1.2 to 3.0 (Morel-Seytoux et al. 1996). This is expected due to the narrow grain-size distribution of the sand. More information on the parameters α_v and n_v can be found elsewhere (van Genuchten 1980; Boufadel et al. 1998, 1999c; Naba et al. 2002).

Tide Simulation

The tide was simulated by pumping water in and out of the tank periodically. The tide can be viewed as a shallow wave in which the horizontal velocity of the water is approximately uniform with depth (Dean and Darlymple 1984). The uniform velocity was simulated with two manifolds placed vertically on each of the long sides of the tank (Fig. 1). The flow of water in and out of the tank was through the manifolds and was driven by two pumps and one three-way solenoid valve. The outflowing water from the wave tank was wasted to the drain.

The height of the simulated tide varied between 70 and 110 cm with a tidal period of about 37.5 min. Because the beach slope in the intertidal zone was 10%, the horizontal distance between the screen and the tide line (i.e., the intersection of the seawater level and the beach surface) was 50 cm at high tide and 450 cm at low tide. Thus, the horizontal extent of the intertidal zone was 400 cm.

Sensors

The experiments required the measurements of the water levels and the concentration of salt. The open water level on the sea side of the tank was measured using a wave gauge (WG) (Model No. LV5900, Omega Engineering) with an accuracy of 1.0 mm. The readings of the WG were logged with Strawberry Tree data soft-

Table 1. Locations of Pressure, Water Level, and Concentration Sensors

Sensor	<i>x</i> (cm)	<i>z</i> (cm)	<i>y</i> (cm)
PT1 ^a	-15	3	60
PT2	78	3	60
PT3	147	3	60
PT4	235.5	3	60
WG	520	NA	30
CM1	59	33.5	20
CM2	54.5	72	45
CM3	118	32	40
CM4	147	67	15
CM5	177	30.5	50
CM6	190	53	30
CM7	220	57	50
CM8 ^a	-15	40	30
CM9	78	94	15
CM10	181	85	10

Note: *x*=horizontal distance from the screen (positive seaward); *z*=elevation from bottom of tank; *y*=horizontal depth from the Plexiglas wall (positive inward perpendicular to the plan of Fig. 1); and NA=not applicable.

^aSensor is landward of screen.

ware (Strawberry Software Inc., Calif.). Four pressure transducers (PTs) (Model No. 1151AP, Fisher) placed at the bottom of the tank measured the water level behind the screen and in the beach. The PTs were accurate to 2.0 mm, and their readings were logged with Strawberry Tree data software, which was also used to control the water level in the tank by sending the appropriate electronic signal to the inflow and the outflow pumps. The locations of the water level devices are given in Table 1 and shown in Fig. 1.

The concentration of the salt was measured by conductivity meters (CMs) (CDCN 108, Omega Engineering). The readings of the CMs were logged with CR10 data software (Rocktest, Inc., Plattsburg, N.Y.). The accuracy of the CMs was about 5% of the measured salt concentration, and the CMs were shaped like hollow disks (doughnuts) with dimensions 10 × 2.5 cm × 3 cm, representing the exterior diameter, the interior diameter, and the thickness, respectively. Early experimentation with the sensors showed that they were not reliable when in contact with sand, and so each CM was placed in a special casing made of Plexiglas. The casings were slotted on all sides and covered with a stainless mesh of hole size about 0.1 mm.

The locations of the probes along the length of the tank are listed in Table 1 and shown in Fig. 1. The horizontal distances of the CMs from the Plexiglas wall were different to minimize the effects of the sensors on one another along the general flow direction (landward-seaward).

Tracer Application

Two duplicate experiments were conducted using NaCl as a conservative tracer. For each experiment, the NaCl solution was obtained by dissolving 261 g of sodium chloride in 100 L of tap water, which had a salinity (ion content converted to salinity) of about 0.15 g/L. To ensure cyclic conditions, at least two tidal cycles were allowed to occur prior to applying the tracer solution at low tide. The solution was added onto the beach surface at the location *x*=126 cm, corresponding to a beach elevation of

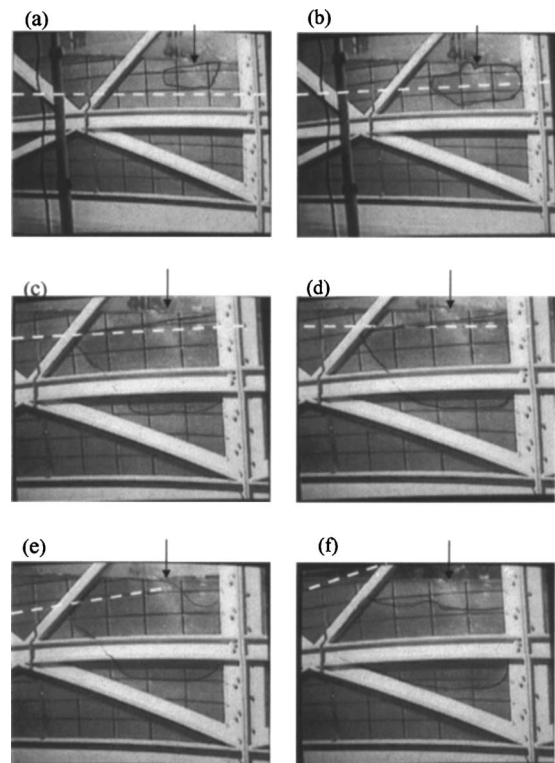


Fig. 2. Snapshot of dye plume at various times, indicating that plume fills intertidal zone initially, then moves landward (right to left) and downward during rising tides. WL at PT3=dashed line: (a) $t=22$ min (2 min into application), WL=92.7 cm; (b) $t=24$ min (4 min into application), WL=93.4 cm; (c) $t=31$ min (11 min into application), WL=94.9 cm; (d) $t=36$ min (16 min into application), end of application, WL=95.6 cm; (e) $t=51$ min (15 min after end of application), WL=95.7 cm; and (f) $t=57$ min, high tide, WL=109.96 cm. Vertical arrow indicates application location of tracer solution; top of U-shaped horizontal beam on side wall of tank is at elevation 70 cm.

$z=103$ cm (Fig. 1). A half-inch perforated manifold was used to spread the solution across the width of the tank. Local ponding occurred during application of the solution, which caused the tracer to spread longitudinally on the beach surface to about 5 cm landward and seaward of the application point. The application took about 16 min and then the tidal cycle was started again. The time zero reported here corresponds to the high tide that occurred prior to tracer application. Thus, the tracer application started at time $t=20$ min and ended at $t=36$ min. The data from all the sensors were logged at an interval of 30 s.

Results

To visualize the overall motion of the plume, an experiment was conducted using 50 g of rhodamine dye instead of NaCl as a tracer. The experiment was conducted as if the tracer were NaCl. The dye adsorbs to the sand and hence its motion is expected to be slower than NaCl, but it is used solely to provide a qualitative description of the transport in the beach. Fig. 2 shows the dye plume at various times, where the edge of the plume is traced using a pencil (in case a black and white copy is made of the colored photographs). The water table obtained from the pressure transducers' readings is plotted as a dashed line; the elevation of

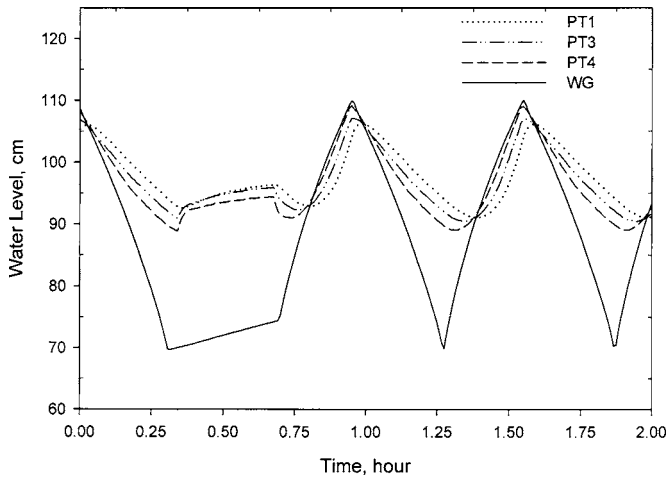


Fig. 3. Variation of water levels with tide; beach water table lags behind falling tides because beach fills faster than it drains

the water table in Fig. 2 is approximate due to distortion of the camera's view.

The dye plume moved downward initially [Fig. 2(a)] until it hit the water table and started spreading in the longitudinal direction of the tank (landward-seaward), as shown in Fig. 2(b). After 11 min of application, the plume had propagated downward to the elevation of 50 cm beneath the injection area [Fig. 2(c)]. The extent of the plume at the end of application ($t=36$ min) is reported in Fig. 2(d). At later times, the shape and spatial extent did not change much until the rising tide level approached the elevation 95 cm [Fig. 2(e)], where the plume moved landward, as can be noted by comparing the landward edge of the plume to Fig. 2(d). The landward displacement continued until high tide [Fig. 2(f)] and was accompanied by a downward displacement, as can be noted by comparing the lower edges of the plumes between Figs. 2(e and f).

Also noted in Fig. 2(f) is a near-surface zone, about 20 cm deep, that is devoid of any dye tracer. The picture of the plume did not change during the falling tide (not reported). Hence, it appears that a rising tide causes a predominantly downward motion of a plume located in the intertidal zone. The tracer study with NaCl (in the remainder of the paper) demonstrates that the applied plume moves seaward during falling tides. For the NaCl experiments, the results of the duplicate experiments were essentially the same, as can be noted by comparing the figures on pages 280 and 282 of Boufadel (1998). For this reason, we report the results of one experiment: Run 4_27 of Boufadel (1998).

Fig. 3 reports the variation of the water levels with time starting from a high tide. As the tide level drops, the most seaward transmitter (PT4) responded first, followed by PT3 and PT1 (PT2 was not functioning correctly). The water level in the beach rose during tracer application, with the level at PT1 equal essentially to that of PT3. In the following times, one can clearly note the delayed response of the beach during falling tides. Further discussion about the laboratory beach hydraulics during and after tracer application is reported in Boufadel et al. (1998), which used a numerical model for variably saturated flow in porous media.

Fig. 4 reports the concentration variation with time at CM9 and CM10, along with the water pressure at PT3, representing the beach water table at $x=147$ cm. The figure shows that the concentration increased first at CM9, then at CM10. Both CMs reached the maximum concentration (within instrument's accu-

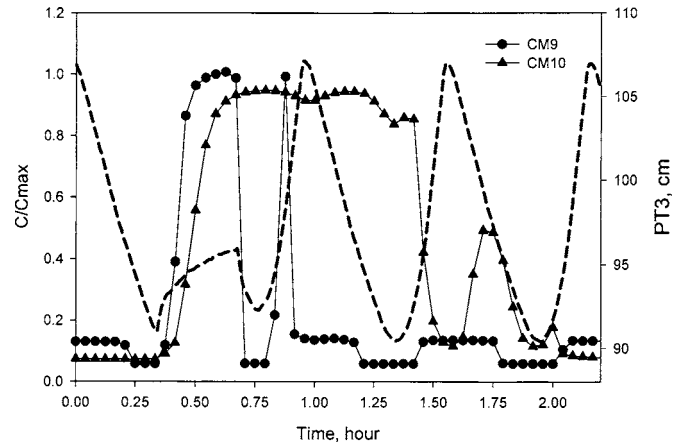


Fig. 4. Variation with time of concentration near injection location. Values are normalized by dividing by $C_{max}=2.76$ g/L; tidal period is 0.67 h; dashed line represents PT3 (water table)

racy) of about 2.76 g/L. The concentration at CM9 dropped immediately following the end of the injection, due to the fact that the water level at PT3 dropped below 94.0 cm, the elevation of CM9. This caused the sensor to be exposed to air (within the casing) and to give a reading of zero (the CMs were calibrated to give a zero reading in air). The concentration at this sensor reached the maximum value as soon as the sensor became submerged in the following tide ($t \approx 0.85$ h).

The effects of water submergence on CM9 are also apparent during the following cycles, where the sensor's concentration dropped to zero whenever the water level was below the sensor and rose sharply to the background value whenever the sensor was submerged. The concentration at CM10, which is at the elevation of 85 cm, persisted for a longer time because the sensor remained submerged (the lowest value of the water table, PT3, was about 90 cm). The concentration at CM10 decreased during rising tides and increased during falling tides. The decrease indicates a downward motion of the plume [Fig. 2(d)]. The increase indicates a seaward motion, because the injection was landward of CM10.

Fig. 5 reports the concentration readings of CM4, CM6, and CM7, along with PT3. The concentration at CM4 increased steadily due to the injection and remained at the maximum value for about four tidal cycles, decreasing to the background value in the following two cycles. Meter CM6 increased a little during the injection, and CM7 remained at the background value. For both CM6 and CM7, the concentration increased during falling tides and decreased during rising tides. This observation, along with the fact that CM4 decreased while CM6 and CM7 increased, indicates a predominant seaward motion of the plume accompanied by a downward motion.

Fig. 6 reports the concentration readings of CM1, CM2, CM3, and CM5. The concentration at CM2 rose first during the rising tide that followed the injection, indicating that the plume in the upper part of the beach moved landward. The pattern of CM2 is opposed to those of CM10, CM6, and CM7, in that it was increasing during rising tides and decreasing during falling tides, probably because CM2 was essentially landward of the intertidal zone (Fig. 1). The highest concentration value at this sensor was about 40% of the maximum. The decrease in the concentration at CM2 coincided with increases in the concentrations at CM3 and CM5. For these two sensors, most of the change in concentration occurred during falling tides. The rising tides slowed the increase in

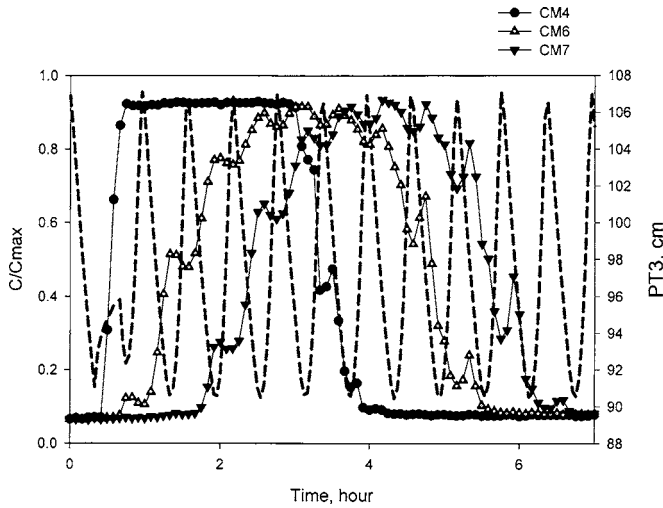


Fig. 5. Variation with time of concentration at sensors at intermediate depth in beach, $C_{\max}=2.76$ g/L; tidal period is 0.67 h; dashed line represents PT3 (water table); time series indicates downward-seaward motion

concentration in the rising limbs of CM3 and CM5 and the decrease in concentration in the falling limbs. The concentration at CM1 increased slightly at latter times.

An integral means to quantify the overall motion of the plume is tracking the variation of the centroid of the plume with time. The coordinates of the centroid of the plume are given by

$$X_G = \frac{M_{x,1}}{M_{x,0}} \quad (1a)$$

$$Z_G = \frac{M_{z,1}}{M_{z,0}} \quad (1b)$$

where M represents the spatial moment in the x - or z -direction

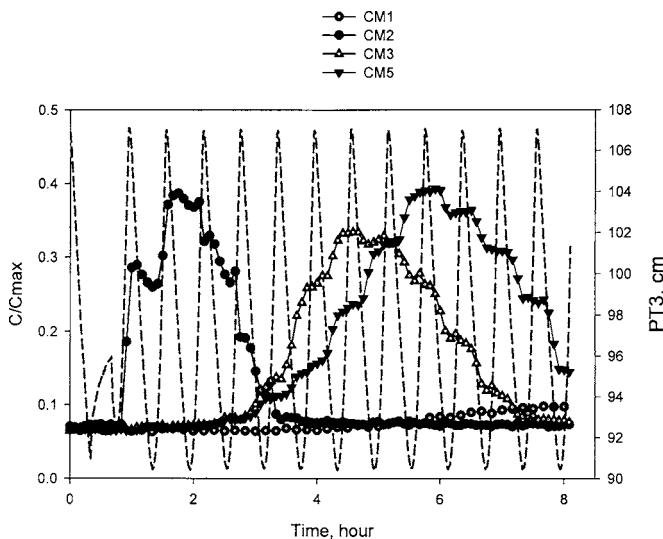


Fig. 6. Variation with time of concentration at most landward sensor (CM2) and lowest sensors (CM1, CM3, CM5); $C_{\max}=2.76$ g/L; tidal period is 0.67 h; dashed line represents PT3 (water table); time series indicates downward overall motion and landward motion for sensors landward of intertidal zone (CM1 and CM2)

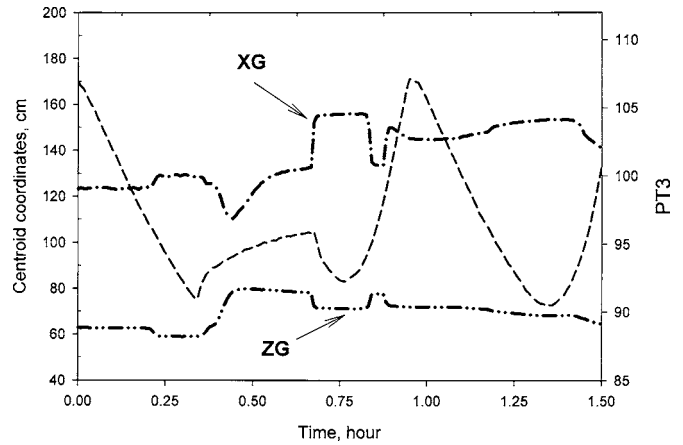


Fig. 7. Temporal variation of coordinates of plume centroid for $t \leq 1.5$ h; increase in X_G indicates seaward movement; decrease in Z_G indicates downward movement; dashed line represents PT3 (water table)

$$M_{s,q} = \sum_{i=1}^{nc} s_i^q c_i \quad (2)$$

where $s=x, z$; and nc =total number of concentration sensors used to compute the moments; $nc=9$ herein, because the measurements of CM8 were always at the background level and thus were not used. Recall that the origin for Fig. 1 ($x=0, z=0$) is at the bottom left of the tank, at the screen. Hence, an increase in X_G represents a seaward movement of the plume and a decrease in Z_G indicates a downward movement.

Prior to the injection, the concentration in the tank was uniform at the background value 0.15 g/L. Hence, upon substitution in Eqs. (1) and (2), one obtains the coordinates of the centroid at time zero ($X_{G_0} \approx 120$ m, $Z_{G_0} \approx 60$ cm). Fig. 7 reports X_G, Z_G , and the water level at PT3 as a function of time. During the injection, Z_G increased by about 20 cm, due to the introduced high concentrations in the upper part of the beach (CM9). The quantity X_G decreased initially because CM9 is more landward than X_{G_0} , and it was the first CM to respond to the injection of the solution (Fig. 4). Thus X_G started increasing about 6.0 min after the beginning of injection because the concentration at CM10, which is seaward of X_{G_0} , increased. Immediately after the end of injection, a sudden increase in the centroid location is noted, due to the fact that the water level dropped below the elevation of CM9, causing this sensor to give a zero reading; hence the centroid shifted seaward. The effect of submersion (or its lack) on CM9 becomes negligible after $t=1.0$ h.

At $t=4.20$ h (Fig. 8), the net seaward transport was about 60 cm ($180-120=60$ cm), and the net downward transport was about 10 cm ($60-50=10$ cm). If one elects to consider the extrema of the centroid's coordinates, one finds a maximum seaward transport of 70 cm ($180-111 \approx 70$ cm) and a net vertical transport of ($75-50=25$ cm). In all cases, the seaward transport of the centroid seems to be between three- and fourfold the downward transport.

Discussion

Flow and Transport in Beach

The tidal amplitude was assumed constant in this study while it varies on natural beaches, depending on the moon; the maximum

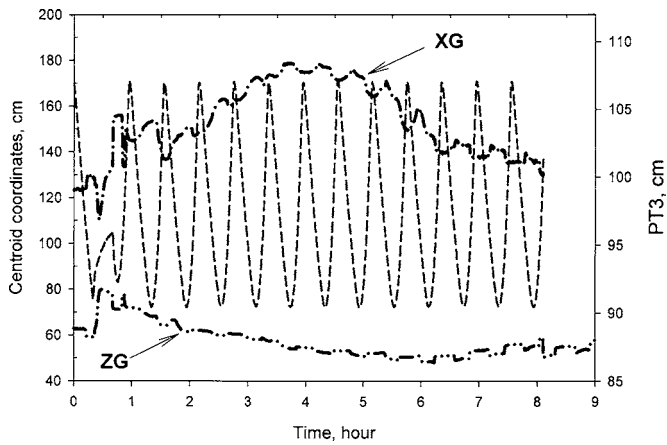


Fig. 8. Variation of coordinates of plume centroid as function of time for duration of experiment; seaward motion of plume persisted for about $t=4.5$ h; downward motion of plume persisted for about $t=6.0$ h; dashed line represents PT3 (water table)

tidal amplitude occurs at a full moon (spring tide) while the minimum tidal amplitude occurs at a quarter moon (neap tide). The use of a constant tidal amplitude in this study was adequate because a tracer study by Wrenn et al. (1997a,b) revealed that although the lunar cycle affects the washout rate from the beach, it does not alter the washout trajectory.

The experiments in this study were designed such that the landward water table (simulated by the water volume landward of the screen, in Fig. 1) rose and dropped in response to the tide. This situation occurs in natural beaches, with hydrologic divides separating the water table in the beach from the regional water table. If such a hydrologic divide is not present, the washout rate to sea is expected to be larger, because the regional water table is higher than the mean sea water level.

The vertical flux of water in porous media with density gradients due to dilute concentrations is given by Boufadel et al. (1999b)

$$q_z = -K \left(\frac{\rho}{\rho_0} + \frac{\partial \psi}{\partial z} \right) = \left[-K \frac{\Delta \rho}{\rho_0} \right] + \left[-K \left(1 + \frac{\partial \psi}{\partial z} \right) \right] \quad (3)$$

where z =positive upward; ψ =pressure head; K =hydraulic conductivity; ρ_0 =density of the background solution (tap water in our case); ρ =density of the actual solution; and $\Delta \rho = \rho - \rho_0$. The second bracket on the right-hand side of Eq. (3) represents the vertical flow due to a neutrally buoyant plume, which depends on the overall hydraulics of the systems and could be positive (upward) or negative (downward). The first bracketed term represents the vertical flow due to density gradients; it is negative (downward) if $\Delta \rho \gg 0$ (in this study). The average velocity for water in the pores is called the linear velocity and is obtained by dividing the Darcy flux by the porosity

$$v = - \frac{K \Delta \rho}{\phi \rho_0} \quad (4)$$

Noting that for this study $K=0.2$ cm/s, the downward velocity is equal to $v \approx 6.3$ cm/h. Hence, in a total duration of 5 h, Eq. (4) predicts that the plume moves about 30 cm downward. This indeed is observed in Fig. 8. We are reluctant to accept that the downward transport of the plume was due solely to negative buoyancy for the following four reasons.

First, in Wrenn et al. (1997a,b), a naturally buoyant tracer solution did indeed move downward (freshwater was used to make the solution, such that the density of the applied solution was equal to that of seawater at the natural beach). Second, the dye tracer experiment showed that the dye is flushed downward in the beach during a rising tide [compare Figs. 2(e and f)]. Considering that the top 20 cm of the beach were cleared of dye under high tide and that the tidal half-cycle is about 19 min, the downward velocity of the plume is about 60 cm/h. This value is 50 times that given by Eq. (4) for the dye tracer, whose concentration was 0.5 g/L.

Third, in the tracer study using NaCl, the concentration at most sensors (Figs. 4–6) and the vertical coordinate of the centroid (Fig. 8) were changing in response to the tide, and not independently of it, as Eq. (4) implies. The reason for the downward displacement of the plume during a rising tide is that the tide fills the beach at a downward angle and not horizontally. This is because the submerged beach surface is equipotential, and subsequently, velocity vectors are perpendicular to it (Boufadel 2000). Considering that the beach slope is 10%, the velocity of water entering the beach from the seaside was essentially vertical.

Fourth, Boufadel (2000) conducted experiments in the same laboratory setup subjected to the same tidal period and amplitude as in this study. They modeled the experiments using the MARUN model (Boufadel et al. 1999b), a finite-element code for density-and-viscosity-dependent flows in variably saturated media, and found no discernible density gradients in experiments where the maximum difference in concentration was the same as in this study (2.61 g/L). Their experiments, however, started by filling the beach with the tracer (NaCl) and subjecting the beach to tide. In addition, the beach properties were different than those in this study, and a high-water table landward of the beach was maintained during the experiments. In summary, buoyancy effects were not the major reason for the downward displacement of the plume.

It is important to note that during a rising tide, seawater could enter the beach even if the tide level is below the beach water table. This occurs if the rising speed of the tide is larger than a critical rise speed that depends on beach material. Simply put, if the tide rises fast and the beach is highly permeable, then water continues to flow seaward, whereas if the beach has a low permeability, then water would enter the beach. Boufadel and Peridier (2002) considered a vertical-face beach and developed a closed-form solution for the critical speed as a function of beach properties. For inclined beaches, no exact solution is available, but the critical speed is lower than that for vertical beaches, as we found based on numerical results (unpublished work).

Scaling Up

The dimensionless approach of Boufadel et al. (1998) can be used to scale up the results of this study. The approach proves that scaling down requires a coarser porous medium in the small scale, which explains the coarse sand used in this study. Boufadel's formulation requires that one conserves three dimensionless quantities between two domains to obtain essentially the same hydraulics. The parameters are M , CF_o , and τ

$$M = \frac{K_{x0}}{K_{z0}} \left(\frac{L_z}{L_x} \right)^2 \quad (5)$$

where K_{x0} and K_{z0} =saturated horizontal and vertical hydraulic conductivities, respectively; and L_z and L_x =vertical and horizontal dimensions of the beach, respectively. Anisotropy in beaches

Table 2. Design Parameters for Prototype and Physical Model

Parameter	Prototype (real beach)	Physical model (laboratory beach)
L_x (m)	43.7	6.3
L_z (m)	5.64	1.15
K_{x0} (cm·s ⁻¹)	0.1	0.2
K_{z0} (cm·s ⁻¹)	0.05	0.2
CF (cm)	32.0	6.45
T (tidal period) (h)	12.25	0.62

could be due to alternating microscopic layers of fine and coarse sand (Waddell 1976). The parameter M combines the aspect ratio with the anisotropy ratio, and the parameter CF_o is given by

$$CF_o = \frac{CF}{L_z} \quad (6)$$

where CF =height of the capillary fringe of the domain, and hence CF_o =dimensionless capillary fringe. The parameter τ is given by

$$\tau = \frac{T}{\frac{L_z}{K_{z0}}} \quad (7)$$

where T =tidal period. The quantity L_z/K_{z0} represents the time it would take the water table to drop the vertical distance L_z if it were moving at the speed K_{z0} . Eq. (7) indicates that τ represents a dimensionless tidal period.

Now consider that one is dealing with a natural beach (prototype) whose properties are reported in Table 2. Its dimensionless parameters take the values $M=0.0333$, $CF_o=0.056$, and $\tau=3.91$. For obvious reasons, these values are the same as obtained from the laboratory beach (model). This indicates, for example, that the tidal amplitude of 0.4 m in the model represents an amplitude of $0.40(5.64/1.15) \approx 2.0$ m in the prototype. The locations of the sensors in the laboratory beach can be converted to the natural beach by multiplying by the ratios of lengths of the prototype to the physical model. Boufadel et al. (1999b) further discuss Boufadel's dimensionless formulation.

Bioremediation

The addition of the tracer to the beach was presented as a variant of the nutrient application strategy used by Venosa et al. (1996). The stoppage of the tide was intended to ensure that the tracer occupied most of the intertidal zone. However, the subsequent hydraulics in the system appear to be independent of the application period, as noted in Fig. 3.

An important mechanism observed in this study was that the downward movement of the tracer plume occurred during a rising tide rather than a falling tide. In this mechanism, water from the sea enters the beach perpendicular to the beach surface, thereby flushing the tracer plume downward, and thus implying that little or no amount of applied dissolved nutrients will be present in the bioremediation zone following a high tide. Therefore, one concludes that dissolved nutrients have to be applied onto the beach at every low tide to maintain maximum microbial growth. This might not be case, however, if slow-release fertilizers are used, an approach that we are currently investigating.

An important goal of bioremediation of oil spills on beaches is ensuring the presence of sufficient amounts of nutrients in the intertidal zone at low tide. Venosa et al. (1996) delivered the

nutrients to the bioremediation zone via a sprinkler system that covered a large landward-seaward distance (10 m). The application strategy used in this study is less labor intensive and demonstrates that it suffices to apply the nutrients at one location near the high tide line. This is because the concentration at CM9 and CM10 remained high prior to the rising of the first tide.

The volume has to be large enough to fill the unsaturated portion of the beach. To obtain such a volume for the prototype, we compute the area of the unsaturated wedge formed at low tide, whose sides are the water table, the beach surface, and a vertical line at the high-tide line. If one notes that the water level at PT1 and PT4 remains higher than 95 and 90 cm, respectively, one finds a triangle whose height is 0.2 m with a side length of 2.5 m (the intertidal zone). By scaling up to the prototype, the dimensions become height ≈ 1.0 m and side length ≈ 17.5 m. Assuming a porosity of 0.33, and recalling that the capillary fringe of the prototype is about 0.30 m, the volume available for water is about 2 m³ per meter parallel to the shoreline. Such a volume of water can be easily pumped from the sea and applied within 1 to 2 h (i.e., in the early stages of a rising tide).

This study assumed that the amount of nutrients consumed by the microorganisms is much smaller than that provided. This assumption is reasonable because the concentration of applied nutrients on natural beaches is usually two orders of magnitude higher than that needed for maximum microbial growth (Venosa et al. 1996).

Acknowledgments

This work was supported in part by the U.S. Environmental Protection Agency's National Risk Management Research Laboratory, in Cincinnati, under Cooperative Agreement No. CR-821029. However, it does not necessarily reflect the views of the agency, and no official endorsement should be inferred.

References

- Bear, J. (1972). *Dynamics of fluids in porous media*, Elsevier, New York.
- Boufadel, M. C. (1998). "The transport of nutrients in beaches: Effect of tides, waves, and buoyancy." Ph.D. thesis, Dept. of Civil and Environmental Engineering, Univ. of Cincinnati, Cincinnati.
- Boufadel, M. C. (2000). "A mechanistic study of nonlinear solute transport in a groundwater-surface water system under steady-state and transient hydraulic conditions." *Water Resour. Res.*, 36, 2549–2566.
- Boufadel, M. C., et al. (1999a). "Optimal nitrate concentration for the biodegradation of *n*-heptadecane in a variably-saturated sand column." *Environ. Technol.*, 20, 191–199.
- Boufadel, M. C., and Peridier, V. (2002). "Exact analytical expressions for the piezometric profile and water exchange between streamwater and groundwater during and after a uniform rise of the stream level." *Water Resour. Res.*, 38(7), 211–218.
- Boufadel, M. C., Suidan, M. T., Rauch, C. H., Venosa, A. D., and Biswas, P. (1998). "2D variably saturated flows: Physical scaling and Bayesian estimation." *J. Hydrologic Eng.*, 3(4), 223–231.
- Boufadel, M. C., Suidan, M. T., and Venosa, A. D. (1999b). "A numerical model for density-and-viscosity-dependent flows in two-dimensional variably-saturated porous media." *J. Contam. Hydrol.*, 37, 1–20.
- Boufadel, M. C., Suidan, M. T., Venosa, A. D., and Bowers, M. T. (1999c). "Steady seepage in trenches and dams: Effect of capillary flow." *J. Hydraul. Eng.*, 125(3), 286–294.
- Brown, A. C., and McLachlan, A. (1990). *Ecology of sandy shores*, Elsevier, New York.

- Dean, R. G., and Dalrymple, R. A. (1984). *Water wave mechanics for engineers and scientists*, Prentice-Hall, Englewood Cliffs, N.J.
- Frind, E. O. (1982). "Simulation of long-term transient density-dependent transport in groundwater." *Adv. Water Resour.*, 5, 73–88.
- Galeati, G., Gambolati, G., and Neuman, S. P. (1992). "Coupled and partially coupled Eulerian-Lagrangian model of freshwater-seawater mixing." *Water Resour. Res.*, 28, 149–165.
- Glover, R. E. (1959). "The pattern of fresh water flow in coastal aquifers." *J. Geophys. Res.*, 64, 439–475.
- Henry, H. R. (1964). "Effects of dispersion on salt encroachment in coastal aquifers." *U.S. Geological Survey Water Supply Paper 1613-C*, C71–C84.
- Merlin, F.-X., et al. (1995). "Bioremediation: Results of the field trials of Landevennec (France)." *Proc., Int. Oil Spill Conf.*, American Petroleum Institute, Washington, D.C., 917–918.
- Morel-Seytoux, H. J., Meyer, P. D., Nachabe, M., Touma, J., van Genuchten, M. T., and Lenhard, R. J. (1996). "Parameter equivalence for the Brooks-Corey and van Genuchten soil characteristics: Preserving the effective capillary drive." *Water Resour. Res.*, 32, 1251–1258.
- Naba, B., Boufadel, M. C., and Weaver, J. (2002). "The role of capillary forces in steady-state and transient seepage flows." *Ground Water*, 40(4), 407–415.
- Nielsen, P. (1990). "Tidal dynamics of the water table in beaches." *Water Resour. Res.*, 26, 2127–2134.
- Philip, J. R. (1973). "Periodic nonlinear diffusion: An integral relation and its physical consequences." *Aust. J. Phys.*, 26, 513–519.
- Riedl, R. J., Huang, N., and Machan, R. (1972). "The subtidal pump: A mechanism of interstitial water exchange by water action." *Mar. Biol. (Berlin)*, 13, 210–221.
- Rosenberg, E., Legmann, R., Kushmaro, A., Taube, R., Adler, E., and Ron, E. Z. (1992). "Petroleum bioremediation—A multiphase problem." *Biodegradation*, 3, 337–350.
- Safferman, S. I. (1991). "Selection of nutrients to enhance biodegradation for the remediation of oil spilled on beaches." *Proc., Int. Oil Spill Conf.*, American Petroleum Institute, Washington, D.C., 571–576.
- van Genuchten, M. T. (1980). "A closed-form equation for predicting the hydraulic conductivity of unsaturated soils." *Soil Sci. Soc. Am. J.*, 44, 892–898.
- Venosa, A. D., et al. (1996). "Bioremediation of an experimental oil spill on the shoreline of Delaware Bay." *Environ. Sci. Technol.*, 30, 1764–1775.
- Waddell, E. (1976). "Swash-groundwater-beach profile interactions." *Spec. Publ. 24*, Society of Economic Paleontologists and Mineralogists, 115–125.
- Wrenn, B. A., Boufadel, M. C., Suidan, M. T., and Venosa, A. D. (1997a). "Nutrient transport during bioremediation of crude oil contaminated beaches." *4th Int. Symp. on In-situ and On-site Bioremediation*, Battelle, Columbus, Ohio, 267–272.
- Wrenn, B. A., Suidan, M. T., Strohmeier, K. L., Eberhart, B. L., Wilson, G. J., and Venosa, A. D. (1997b). "Nutrient transport during oil-spill bioremediation: Evaluation with lithium as a conservative tracer." *Water Res.*, 31, 515–524.